scientific reports

Check for updates

OPEN

Development of sensitive and accurate solid-phase microextraction procedure for preconcentration of As(III) ions in real samples

Adil Elik[1], Mustafa Tuzen[2,3]✉, Baki Hazer[4,5], Savaş Kaya[6], K. P. Katin[7] & Nail Altunay[8]✉

We synthesized the poly(methyl methacrylate-co-2-aminoethyl methacrylate (PMaema) amphiphilic copolymer in a form of solid phase adsorbent. Then it was used for separation, preconcentration and determination of trace amount of As(III) ions from foods and waters with hydride generation atomic absorption spectrometry. The PMaema was characterized by fourier transform infrared spectrometer and nuclear magnetic resonance spectrometer. The adsorption of As(III) to the PMaema was also supported using computational chemistry studies. The experimental parameters (pH, PMaema amount, adsorption time and ethanol volume) were optimized using a three-level Box–Behnken design with four experimental factors. We observed linear calibration curve for the PMaema amount in the 10–500 ng L^{-1} range ($R^2 = 0.9956$). Limit of detection, preconcentration factor and sorbent capacity of PMaema were equal to 3.3 ng L^{-1}, 100 and 75.8 mg g^{-1}, respectively. The average recoveries (spiked at 50 ng L^{-1}) changes in the range of 91.5–98.6% with acceptable relative standard deviation less than 4.3%. After validation studies, the method was successfully applied for separation, preconcentration and determination of trace amount of As(III) from foods and waters.

Arsenic is known as the toxic element for living organisms even at the ultra-trace levels. It leads to many human health problems, including skin and lung cancer[1]. Irrigation of soil, vegetables and plant crops with arsenic-contaminated water results in accumulation of arsenic in the plants[2]. Then it enters the human bodies through their daily diet.

Arsenic possesses different oxidation states in water, the most common of them are arsenite (As(III)) and arsenate (As(V)). Toxicity of arsenite is higher than arsenate[3,4]. However, arsenic does not have any health benefits either in the arsenite or arsenate forms. This is why it was commonly quantified as the total arsenic level rather than the fractions of individual species[1]. Determination of arsenic in water, food and environmental samples attracts great research interest due to its toxic effects on human and animal health[5,6]. The European Food Safety Authority proposed maximum permissible levels of inorganic arsenic of 100, 200, 250, and 300 μg kg^{-1} for rice cakes, polished and white rice, parboiled rice, wafer cookies, and rice for the production of foods for infants and children, respectively[7,8]. Environmental Protection Agency reduced the permissible standard of arsenic concentration in drinking water from 50 to 10 μg L^{-1}[9]. According to the Turkish Food Codex, the level of arsenic in soft drinks may not exceed 0.1 μg g^{-1}[10].

Various instrumental analytical techniques, such as capillary electrophoresis[11], inductively coupled plasma mass spectrometry (ICP-MS)[12], electrothermal atomic absorption spectrometry (ETAAS)[13–15], inductively

[1]Department of Chemistry, Sivas Cumhuriyet University, 58140 Sivas, Turkey. [2]Faculty of Science and Arts, Chemistry Department, Tokat Gaziosmanpasa University, 60250 Tokat, Turkey. [3]Center for Environment and Water, King Fahd University of Petroleum and Minerals, Research Institute, Dhahran 31261, Saudi Arabia. [4]Department of Aircraft Airframe Engine Maintenance, Kapadokya University, Urgup, 50420 Nevşehir, Turkey. [5]Chemistry Department, Zonguldak Bulent Ecevit University, 67100 Zonguldak, Turkey. [6]Health Services Vocational School, Department of Pharmacy, Sivas Cumhuriyet University, 58140 Sivas, Turkey. [7]Institute of Nanoengineering in Electronics, Spintronics and Photonics, National Research Nuclear University "MEPhI", Kashirskoe Shosse 31, Moscow 115409, Russia. [8]Department of Biochemistry, Sivas Cumhuriyet University, TR-58140 Sivas, Turkey. ✉email: mustafa.tuzen@gop.edu.tr; naltunay@cumhuriyet.edu.tr

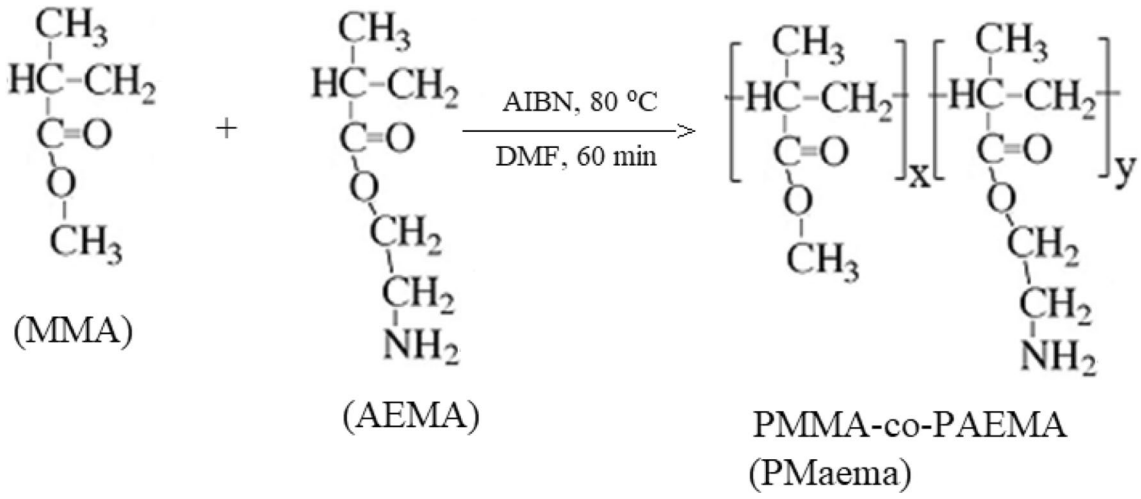

Scheme 1. Reaction design of free radical copolymerization of MMA and AEMA in DMF solution.

coupled plasma optic emission spectrometry (ICP-OES)[16], UV-spectrophotometer[17] and hydride generation atomic absorption spectrometry (HGAAS)[18] are widely used for determination of arsenic in water, food and environmental samples. The HGAAS has some advantages due to its low cost, high sensitivity and reproducibility. To detect arsenic in very low (trace and ultra-trace) concentrations in water and food samples using HGAAS, separation and preconcentration steps are necessary. Various separation and preconcentration methods, such as ultrasonic-assisted micro solid phase extraction[19], hollow fiber liquid phase microextraction[20], dispersive liquid–liquid microextraction[21], enzyme based hydrolytic water phase microextraction method[22], and solid phase microextraction[23] have been proposed for separation and preconcentration of arsenic in different matrices. The advantages of solid phase microextraction over other preconcentration methods are its simplicity, high rate, short extraction time and high preconcentration factor. In addition, the efficiency of solid phase microextraction can be increased by novel recently proposed methods, including surfactant-assisted[24] and ultrasonic-assisted[25] preconcentration and using of N-doped mesoporous carbon-based[26] and magnetized-based[27] materials. These approaches provide faster phase separation during solid phase microextraction.

Recently, we used polystyrene-polydimethyl siloxane hydrophobic copolymer for separation and preconcentration of arsenic ions[28]. In this work, we used a new amphiphilic copolymer with pendant aminoethyl groups. Amphiphilic copolymers contain both hydrophilic and hydrophobic blocks[29,30]. Poly (methyl methacrylate) is a glassy, hydrophobic polymer. Poly (2-aminoethyl methacrylate) (PMaema) hydrochloride is a hydrophilic polymer, which belongs to a promise for gene delivery class of polymers[31]. The 2-aminoethyl methacrylate (Maema) can be (homo/co)polymerized by atom transfer radical polymerization which is a type of controlled living free radical polymerization[32,33]. In this study, Maema was copolymerized with hydrophobic MMA to decrease water solubility. Then, the amphiphilic copolymer poly (methyl methacrylate-co-2-aminoethyl methacrylate) was prepared via conventional free radical polymerization[34]. Prepared copolymer swelled but did not solute in water. We characterized this new copolymer (PMaema) and used it for separation, preconcentration and determination of arsenic ions in water and some food samples.

Results

FTIR and 1H NMR characterization of PMaema. Scheme 1 presents the polymerization reaction yielding to amine functionalized amphiphilic copolymer PMaema.

The characteristic signals of the PMaema copolymer were observed in both FTIR and ^{1}H NMR spectra (Fig. 1a,b). They demonstrated good agreement with the previously reported spectra[35]. FTIR spectrum possessed peaks at 3410, 2021, 1606 and 1608 cm^{-1} (correspond to primary amine of aeMA) and at 1722 cm^{-1} (corresponds to carbonyl of MMA and aeMA). Figure 1a presents the comparative FTIR spectra of the amphiphilic copolymer with the related homopolymers. The characteristic signals of the copolymer can be clearly seen in this comparative FTIR spectra. ^{1}H NMR spectra demonstrated chemical shifts of 4.95, 4.25, 3.65, 3.30 and 0.80/2.00 ppm, corresponding to $-N\mathbf{H}_2$ of aeMA, $-C\mathbf{H}_2-O-$, $-OC\mathbf{H}_3$, $-C\mathbf{H}_2-NH_2$ and $-C\mathbf{H}_2-C(C\mathbf{H}_3)-$ groups, respectively. Ratio of the integral values of the signals at 3.65 and 3.30 ppm shown that the molar concentration of PMaema copolymer in the aema was equal to 29% (see Fig. 1b).

Computational chemistry approach. In our computational study, the PMaema copolymer was represented by the $C_{20}H_{36}N_2O_8$ molecule. We considered three possible geometries of As(III)-$C_{20}H_{36}N_2O_8$ (see Fig. 2a–c). Their characteristics are collected in the Table 1. The adsorption energies between As(III) ion and $C_{20}H_{36}N_2O_8$ molecule were calculated as $E_b = E(C_{20}H_{36}N_2O_8) + E(\mathrm{As(III)}) - E(\mathrm{As(III)} - C_{20}H_{36}N_2O_8$. The geometry presented at Fig. 2b provides the strongest adsorption. In this complex, nitrogen does not interact with the As(III) ion; moreover we observed detachment of the CH_2-NH_2 ligands. However, the role of amino groups is very important: they provide parallel displacement of the nearest PMaema fragments. Therefore, As(III) ion can interact simultaneously with two oxygen atoms (see Fig. 2b).

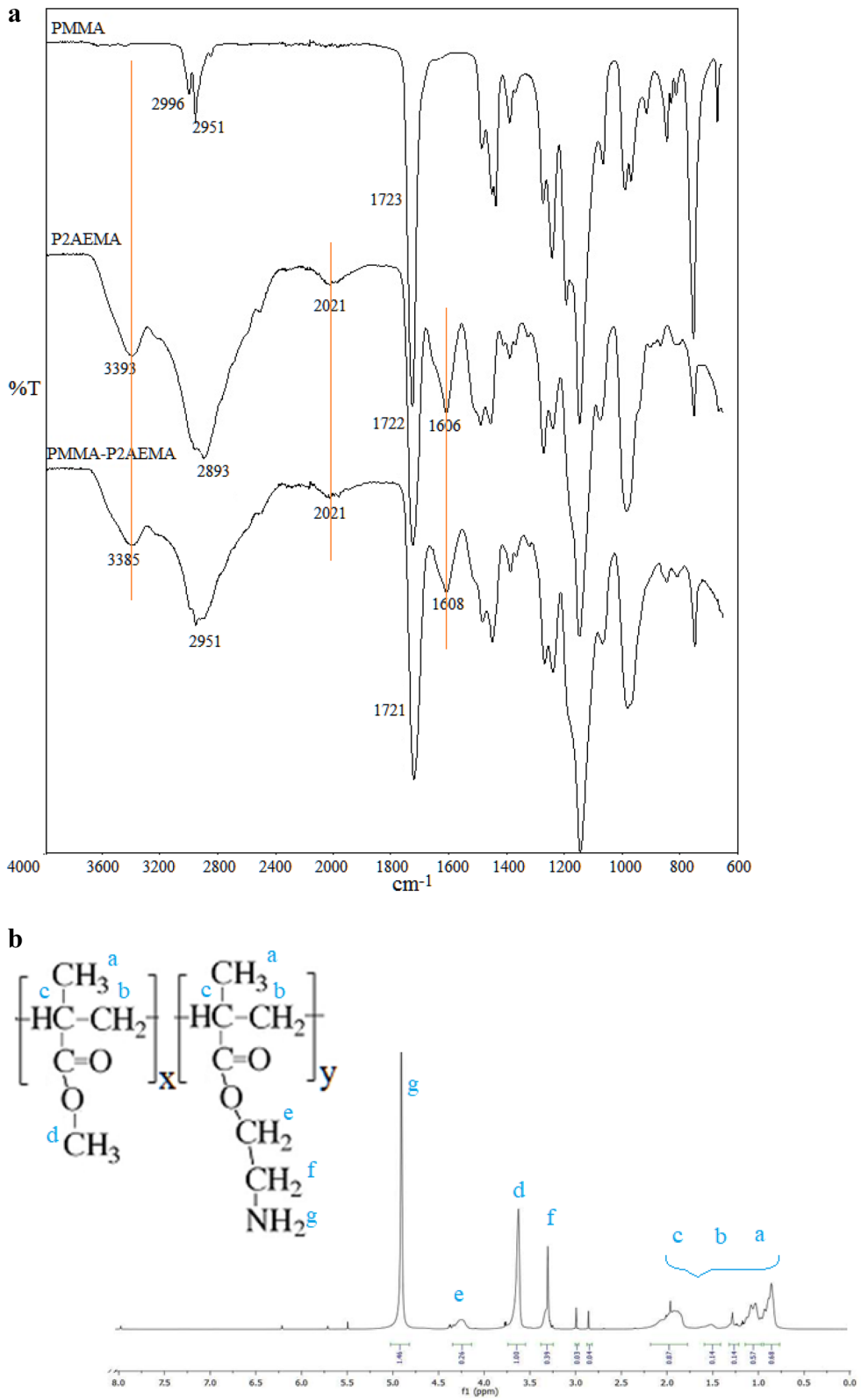

Figure 1. (**a**) FTIR spectra of PMMA, P2AEMA and Poly(MMA-co-AEMA). (**b**) ^{1}H NMR spectrum of the amine functionalized amphiphilic copolymer (PMaema).

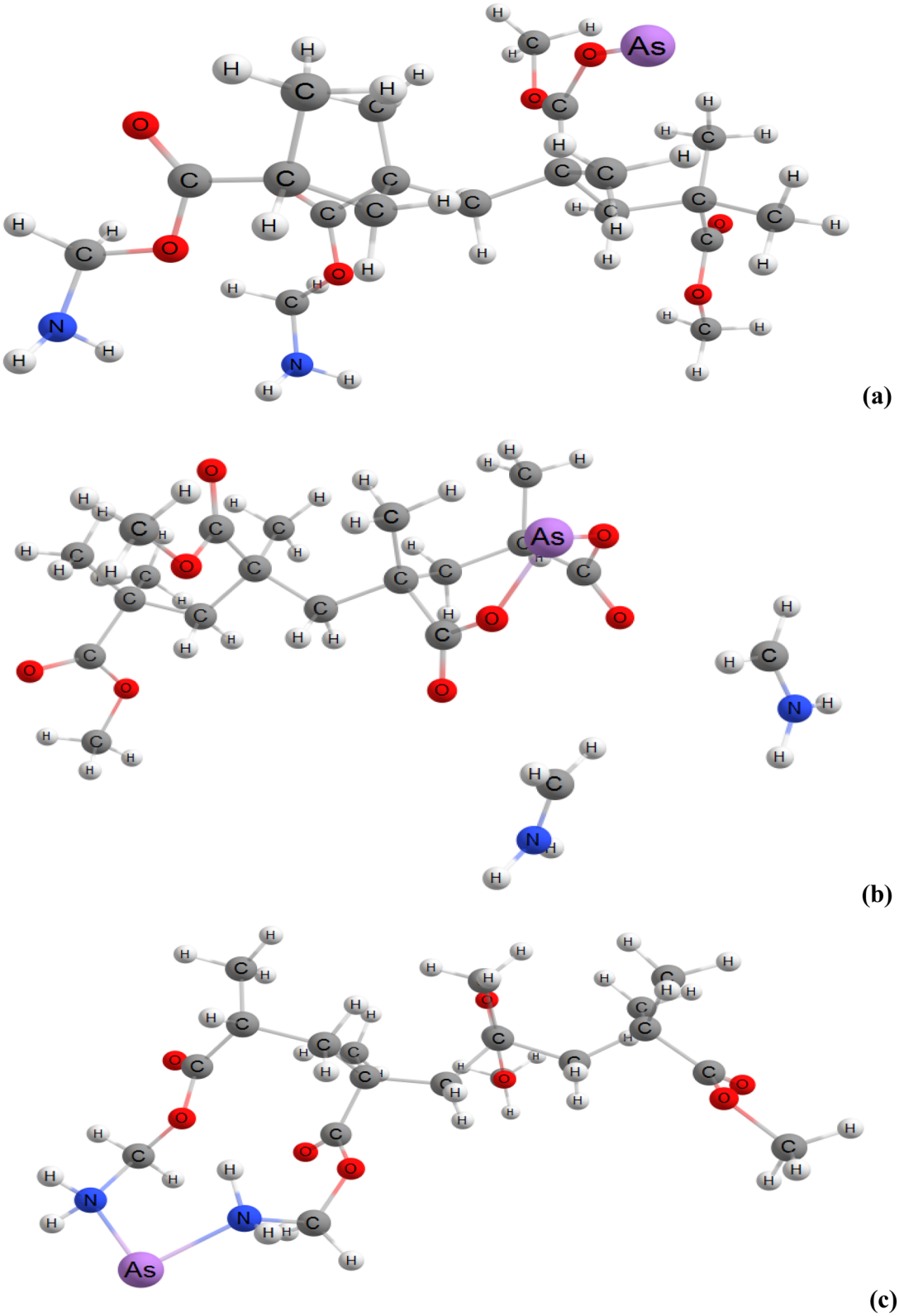

Figure 2. (**a**–**c**) Optimized structures of the As(III)-$C_{20}H_{36}N_2O_8$ complexes.

Chemical hardness of chemical species characterizes their resistance towards electron cloud polarization or deformation. It was introduced by R.G. Pearson[36] is an important indicator of chemical stability. According to maximum hardness principle, hard molecules are more stable compared to soft ones. Some recent applications

System	Charge (|e|)	E_b (eV)	HOMO (eV)	LUMO (eV)	Gap (eV)	Bonds lengths (Å)
$C_{20}H_{36}N_2O_8$	0	–	− 7.15	− 0.39	6.76	–
As(III)–$C_{20}H_{36}N_2O_8$ **(a)**	3	9.56	− 7.70	− 7.20	0.50	$l_{As-O} = 1.781$
As(III)–$C_{20}H_{36}N_2O_8$ **(b)**	3	14.17	− 7.81	− 4.98	2.83	$l_{As-O1} = 1.739$; $l_{As-O2} = 1.752$
As(III)–$C_{20}H_{36}N_2O_8$ **(c)**	3	11.88	− 7.99	− 7.71	0.29	$l_{As-N1} = 1.929$; $l_{As-N2} = 1.976$

Table 1. Calculated characteristics of the $C_{20}H_{36}N_2O_8$ molecule and its complexes with the As(III) ion.

of this principle were presented in detailed in the book edited by Islam and Kaya[37]. According to Table 1, the structure presented in Fig. 2b is harder and more stable compared to others structures. There is an inverse relation between chemical hardness and polarizability. According to the minimum polarizability principle, "in a stable state, the polarizability is minimized." This principle also supports the stability of geometry presented in Fig. 2b. Another indicator of the chemical stability is the electrophilicity index. Minimum electrophilicity principle proposed via Parr's electrophilicity index states: "in a stable state, electrophilicity is minimized." Electrophilicity values calculated in the light of Parr's electrophilicity index are equal to 111, 14.45 and 220 eV, for geometries presented in Fig. 2a–c, respectively. Therefore, the predictions from the minimum electrophilicity, maximum hardness and minimum polarizability principles are in good agreement with each other. All these principles recognized the structure presented in Fig. 2b as the most stable complex among all studied geometries. The adsorption mechanism regarding to this study is as in the Fig. 2b. Calculated values of electro donating and electro accepting powers for this configuration were equal to 0.64 and 4.41 eV, respectively.

In the light of chemical hardness concept introduced by R.G. Pearson[36], the nature of the chemical interactions, reactivity and stability of chemical species can be illuminated. According to chemical structure of the considered PMaema molecule, it is a hard base. Hard and Soft Acid–Base (HSAB) principle implies classification of Lewis acids and bases into hard and soft. According to this classification, As(III) ion belongs to hard acids (see the Table 1 of Ref.[36]). According to HSAB principle, the electrostatic interaction between hard acids and hard bases should be quite strong. This is why the interaction between As(III) ion and PMaema molecule is powerful.

Selection of elution solvent type. The function of the eluent is to transfer the analyte adsorbed on the solid phase into the final solution. However, eluent should not deform the solid adsorbent. We investigated nine different eluents to select the best of them. The recoveries of As(III) ions with using of acetone, THF, acetonitrile, sulfuric acid, water, nitric acid, hydrochloric acid, methanol and ethanol as the eluent were equal to 45.7%, 51.8%, 59.5%, 68.9%, 74.1%, 75.9%, 81.0%, 82.5% and 91.7%, respectively. The highest recovery for As(III) ions was achieved in the presence of ethanol. This is why ethanol was chosen as the preferable eluent for further optimization.

Chemometric approaches. *Statistical analysis.* To achieve an efficient and fast extraction of As(III) ions from the selected samples, the effect of experimental parameters (pH, PMaema amount, adsorption time and ethanol volume) were investigated with the Box-Behnken design. We assumed second-order polynomial dependence of the goal function on experimental parameters and derived corresponding regression coefficients. We also used analysis of variance (ANOVA) for statistical investigation of the significance of each regression coefficient. Based on data presented in Table 2, we obtained quadratic polynomial dependence of recovery on experimental parameters. This dependence includes linear, binary and quadratic terms:

$$\begin{aligned} \textit{Recovery}\ (\%) &= 90.12 - 4.20\,A + 8.52\,B + 9.86\,C + 11.05\,D - 3.20\,AB + 1.40\,AC - 6.20\,AD \\ &\quad + 9.57\,BC - 3.60\,BD + 4.95\,CD - 18.35\,A^2 - 13.24\,B^2 - 14.97\,C^2 - 18.38\,D^2 \end{aligned}$$

The values of R^2 and adjusted-R^2 (0.9875 and 0.9758, respectively) confirm reliability and predictive power of this regression. AVONA analysis suggests the significance of the established design: *F*-value and *p*-value were equal to 84.65 and < 0.0001, respectively. We also calculated the "lack-of-fit" value, which is used in ANOVA to evaluate the significance and authenticity of the established design. The calculated "lack-of-fit" value was equal to 0.6175, much more than the critical value 0.05. This was the additional justification of the validity of proposed regression.

Assessment of significant factors. The 3D response surface plots of As(III) recovery depending on experimental factors are presented in Fig. 3a–f. The adsorption of the analyte to the synthesized PMaema is strongly depends on the pH of the sample solution. The PMaema could hydrolyze in strong acid or alkali. As a result, the recovery of As(III) could be decreased. Therefore, the pH of sample solution was variated in 2.5 to 8.0 range to provide the best preconcentration and determination of the As(III) ions. The pH 4.3 resulted in the highest recovery, see Fig. 3a–c. The amount of PMaema in the sample solution must be sufficient to ensure complete adhesion of As(III) ions on the PMaema. Figure 3a, d and e show the increase of the recovery with the amount of PMaema, if this amount is lower than 110 mg. Further increase of the amount results to decrease of the recovery. Therefore, 110 mg is the optimal amount of PMaema. Adsorption time should be sufficient to complete the adsorption of As(III). We varied the adsorption time in 0 to 30 min range; the highest recovery was achieved at 22 min (see Fig. 3b, d and f). Longer times was not change recovery significantly. The volume of the eluent (ethanol) should

Source	Sum of squares	df	Mean square	F-value	p-value	
Model	9652.55	14	689.47	84.65	< 0.0001	Significant
Linear interaction						
A	211.68	1	211.68	25.99	0.0001	
B	872.11	1	872.11	107.07	< 0.0001	
C	1166.24	1	1166.24	143.18	< 0.0001	
D	1465.23	1	1465.23	179.88	< 0.0001	
Binary interaction						
AB	40.96	1	40.96	5.03	0.0405	
AC	7.84	1	7.84	0.9625	0.3421	
AD	153.76	1	153.76	18.88	0.0006	
BC	366.72	1	366.72	45.02	< 0.0001	
BD	51.84	1	51.84	6.36	0.0234	
CD	98.01	1	98.01	12.03	0.0034	
Square interaction						
A^2	2310.00	1	2310.00	283.60	< 0.0001	
B^2	1202.34	1	1202.34	147.61	< 0.0001	
C^2	1536.01	1	1536.01	188.57	< 0.0001	
D^2	2316.30	1	2316.30	284.37	< 0.0001	
Residual	122.18	15	56.79			
Lack of fit	76.77	10	7.68	0.8454	0.6175	Not significant
Pure error	45.41	5	9.08			
Cor total	9774.73	29				
Std. dev	2.85	R^2		0.9875		
Mean	64.14	Adjusted R^2		0.9758		
C.V. %	4.45	Predicted R^2		0.9481		
		Adeq precision		27.1523		

Table 2. Regression coefficients and ANOVA analysis of the quadratic model calculated with the stepwise method.

be sufficient to provide transforming of the As(III) ions adsorbed on the PMaema into the solution phase. Too low volumes of ethanol does not provide complete desorption, whereas too high volumes result in both low concentration of the As(III) in solution phase and deformation of the solid adsorbent. We varied the ethanol volume in the range 0.2–2.0 mL (see Fig. 3c, e, f). The maximal recovery of the As(III) ions was achieved at 1.5 mL. Therefore, it is the optimal value of ethanol volume.

Optimum conditions. Analytical data obtained as a result of the application of the experimental model were evaluated with the help of the statistical program (BBD design). In this evaluation, the statistical program was commanded to achieve the highest recovery for As(III). In the light of this command, the most suitable values for the variables optimized by the statistical program were produced as follows. The pH, PMaema amount, adsorption time and eluent volume were 4.3, 110 mg, 22 min and 1.5 mL, respectively. The estimated recovery value for As(III) at the optimum conditions selected by the statistical program was 96.69% with desirability of 1.0. In three-replicate experimental studies conducted at selected optimum conditions, the resulting recovery for As(III) were 96.2%, 96.7%, and 95.4%, respectively. For these studies, standard deviation values ranged from 0.8 to 1.2%. It is easily understood from the results that there is a high agreement between the experimental data and the estimated values of the statistical model. As a result, the above values for As(III) ions with high recovery and good fit were chosen as optimized values for the relevant variables in our study.

Reusability of PMaema. Generally, the cost of newly synthesized PMaema directly depends on its reusability. Analysis costs for routine experiments reduces significantly, if the synthesized adsorbent can be used repeatedly. We investigated the reusability of the PMaema copolymer using model solutions contained 40 ng L^{-1} of As(III) under the optimized conditions. As a result of this study, the adsorption feature of the PMaema copolymer was determined to be apparently stable (< 5%) after the sequential application of > 15 cycles of adsorption and desorption of the As(III) ions.

Effect of sample volume. The effect of sample volume on the recovery of the As(III) ion should be investigated to calculate the preconcentration factor (PF) of the proposed method using the optimum conditions. By definition, the PF is the ratio of sample volume to final volume (1.5 mL). We varied the sample volume in the range 10–350 mL, whereas the concentration of As(III) was kept to be equal to 40 ng L^{-1}. It has been observed

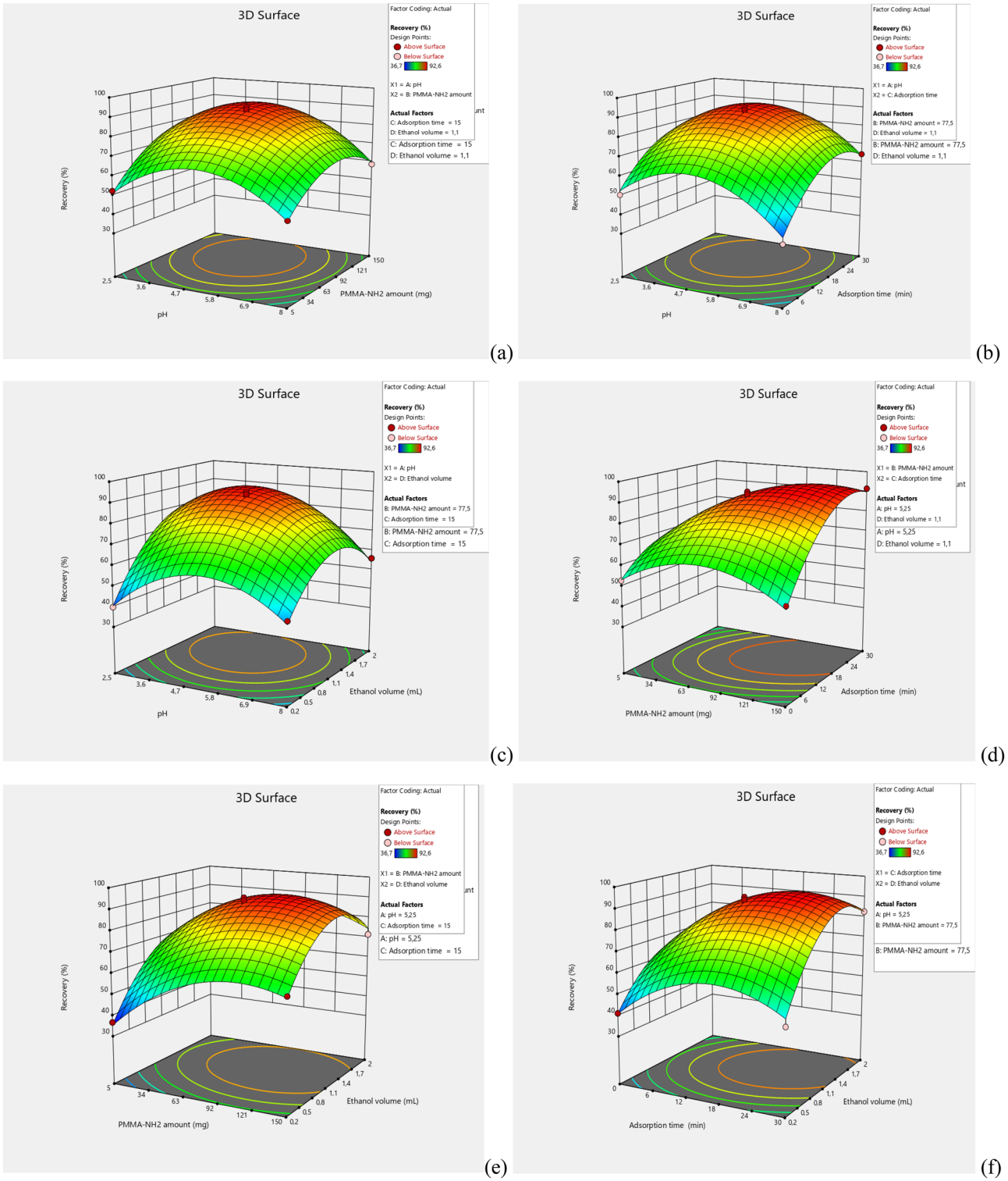

Figure 3. (**a**–**f**) Three-dimensional plot for determination of As(III). (**a**) pH-PMaema amount (mg); (**b**) pH-adsorption time (min); (**c**) ethanol volume (mL)-pH; (**d**) adsorption time (min)- PMaema amount (mg); (**e**) ethanol volume (mL)- PMaema amount (mg); (**f**) adsorption time (min)- ethanol volume (mL).

that the As(III) ions were quantitatively recovered when the sample volume was less than 150 mL. Therefore, 150 mL was adopted as the optimal sample volume. Corresponding value of the PF is equal to 100.

Sorbent capacity. Sorbent capacity was defined as the maximum amount of the analyte retained by one gram of the solid adsorbent. We used the batch adsorption method to determine the sorbent capacity of the PMaema copolymer. In our experiment, 75 mg of the sorbent was added to 50 mL of the model solution contain-

Interfering ions	Tolerance limit[a]	Recovery (%)	RSD (%)
K^+	1500	99.2	2.9
HPO_4^{2-}	1500	98.5	2.6
SCN^-	1500	98.6	3.1
SO_4^{2-}	1000	97.9	2.8
$C_2O_4^{2-}$	1000	98.1	2.9
F^-	1000	98.4	2.7
I^-	1000	98.8	3.1
Zn^{2+}	750	98.2	2.9
Mo^{6+}	750	97.9	2.7
Sb^{3+}	750	97.8	2.5
Mn^{2+}	500	97.0	2.8
Se^{4+}	500	97.4	2.8
Ni^{2+}	500	96.8	2.7
Pb^{2+}	500	96.6	3.1
Co^{2+}	500	97.1	3.4
As^{5+}	250	96.2	3.0
Al^{3+}	250	96.4	3.3
Fe^{3+}	100	95.7	3.5
Mn^{3+}	100	95.1	3.6

Table 3. Tolerance limits of interfering ions for determination of 40 ng L^{-1} As(III) after application method. [a][Interfacing ions]/[As(III)].

ing As(III) ions under the optimum conditions. The mixture was stirred for 20 min to guarantee the achievement of equilibrium. The aqueous portion was then separated by decantation, and the amount of As was measured by HGAAS. The capacity of the sorbent was calculated according to the following formula;

$$Q_e = (C_i - C_e)\, V\, W^{-1} \quad (1)$$

where Qe was the sorbent capacity (mg g^{-1}), Ci and Ce were the initial and final amounts (mg L^{-1}) of As(III) ions, W (g) was the amount of the adsorbent and V (mL) was the volume of the model solution. The maximum sorbent capacity was 75.8 mg g^{-1}. This value indicates that the PMaema copolymer possesses a strong adsorption capability toward the As(III) ions.

Interfering ions. Interfering ions can affect the steps of adsorption of As(III) ions to the PMaema copolymer and cause reducing its sorption efficiency. This was why we tested selectivity of the PMaema using 30 mL of the analyte with model As(III) concentration (40 ng L^{-1}) in the presence of some cations and anions commonly present in the real samples. The tolerance limit was calculated from the ratio of the ions amount, which results in ± 5% relative error in the analytical signal, to the amount of analyte. The recoveries values and tolerance limits are presented in Table 3. The result proves that the interfering ions have no significant effect on the recoveries of As(III) ions.

Analytical performance. Analytical performance characteristics such as linearity, limit of detection (LOD), limit of quantification (LOQ), enrichment factor (EF), relative standard deviation (RSD%) and recovery were investigated under the optimum conditions defined above. These characteristics were determined according to the IUPAC recommendation. The linearity of calibration curve was confirmed from 10 to 500 ng L^{-1} with coefficients correlation $R^2 = 0.9956$. The LOD and LOQ were calculated as $3s_{blank}/m$ and $10s_{blank}/m$, respectively (s_{blank} denotes the standard deviation of the blank solutions, and m stands for the slope of the linear section of the calibration curve). LOD and LOQ were equal to 3.3 ng L^{-1} and 10 ng L^{-1}, respectively. The EF, calculated as the ratio of the slopes of calibration curve before and after microextraction, was equal to 85. The recoveries (spiked at 50 ng L^{-1}) remained in the range of 91.5–98.6% with acceptable RSD% less than 4.3%. Comprehensive results were summarized in Table 4.

Accuracy and precision. The precision was investigated by determining the As(III) in the added rice sample at low (25 ng L^{-1}), middle (150 ng L^{-1}), and high (300 ng L^{-1}) amounts with four repetitions of the sample solution each day. The repeatability was obtained by analyzing the selected rice sample four times during one day, while the reproducibility was obtained by analyzing the selected rice sample four times a day over three consecutive days. The RSDs% for repeatability and reproducibility analysis were lower than 3.6% and 4.1%, respectively. The obtained results were given in Table 5.

In order to assess the accuracy of the optimized method, two standard reference materials (SRMs) such as SRM 1573a (Tomato leaves) and SRM 1568a (Rice flour) were analyzed. The obtained results (see Table 6)

Characteristics	After microextractionn	Before microextraction
Regression equation	A = 0.0513[As(III). ng L^{-1}] + 0.0255	A = 0.0036[As(III). ng L^{-1}] + 0.0016
Correlation coefficient (R^2)	0.9956	0.9914
Linear range (ng L^{-1})	10–500	750–2500
LOD (ng L^{-1})	3.3	227
LOQ (ng L^{-1})	10	750
Recovery (%)	91.5–98.6	85.9–94.3
RSD (%)	4.3	5.6
PF	100	–
EF	85	–
Sorbent capacity (mg g^{-1})	75.8	–

Table 4 . Analytical performance characteristics.

SRMs	Certified value (μg kg^{-1})	Determined (μg kg^{-1})	Recovery (%)	t-test[a]	F-test[a]
1573a (tomato leaves)	112.6 ± 2.4	110.4 ± 3.5	98.0	1.44	2.13
1568a (rice flour)	290 ± 30	281 ± 12	96.9	1.67	4.67

Table 5. Determination of the As in two standard reference materials after application method (N:5). [a]Theoretical value for t- and F-values for 5 degrees of freedom and 95% confidence limits are 2.57 and 6.39 respectively.

	Repeatability (N:4)			Reproducibility (N:4 × 3)		
	Low	Middle	High	Low	Middle	High
RSD (%)	3.5	3.3	3.9	3.7	4.1	4.0
Recovery (%)	94.1	96.9	98.3	92.8	95.6	97.1

Table 6. Repeatability and reproducibility studies for the precision of the application method.

revealed no significant difference at 95% confidence confirming the accuracy of the method. On the other hand, the precision of the method was validated by applying *F*-test and *t*-test at a 95% confidence level. In all cases, the F_{exp} and t_{exp} were found lower than the $F_{theoretical}$ and $t_{theoretical}$.

Analytical applications. In the present study, the total amount of inorganic arsenic was determined as the equivalent of As(III) in the selected samples. In this context, the reduction study of As(V) to As(III) was conducted according to the reported in the literature[38]. A 1.0 mL of solution containing 0.75 g potassium iodide and 1.25 g ascorbic acid was added to 30 mL of sample solutions. To complete reduction, the resulting mixture was left at room conditions for 30 min. After the reduction of As(V), the proposed method was applied for the preconcentration and determination of total inorganic arsenic in foods (rice, brown rice, carrot, pepper, flour, milk powder, tomato, cabbage, garlic, chicken liver and fish) and water samples (tap water, well water, river water, waste water, and bottled water) with a standard addition approach. Analytical results obtained from the analysis of food samples were presented in Table 7. Arsenic could not be detected in two selected food samples including milk powder and garlic. The highest arsenic content was detected in brown rice (114.8 μg kg^{-1}). Recovery values were ranged from 94.2 to 103.2%. The RSDs% were less than 3.7%. These values demonstrate the applicability of the method and independence of the results on matrix effect of the foods.

All water samples were through 0.22 μm cellulose membrane filters (Millipore) prior to their microextraction procedure. analytical results including the recovery and RSDs% in different waters were given in Table 8. While no arsenic was detected in bottled water, tap water and river water, 45.1 ng L^{-1} and 98.5 ng L^{-1} arsenic were determined in well water and wastewater, respectively. Recovery for all water samples was in the range 95.6–103.7% with RSD lower than 3.4%.

Method performances comparison. Performance of the proposed method was compared with some of the previously reported analytical techniques. As can be seen from Table 9, compared to the same HGAAS determination with different microextraction procedure like CPE, DLLME, DES-VAME, our method provides higher PF, lower LOD and wider linearity. This may be due to the high selectivity of the synthesized PMaema amphiphilic copolymer toward As(III) ions and performed BBD optimization. Note that we took into account binary and

Sample	Spiked	Determined (μg kg^{-1})	Recovery (%)	RSD (%)
Rice	–	96.7	–	2.4
	100	192.1	95.4	2.5
Brown rice	–	114.8	–	3.1
	100	216.9	102.1	3.4
Carrot	–	2.7	–	3.2
	100	99.5	96.8	2.8
Pepper	–	54.8	–	2.6
	100	152.5	97.7	2.7
Flour	–	33.6	–	2.1
	100	136.8	103.2	3.3
Milk powder	–	ND[a]	–	3.5
	100	97.5	97.5	3.7
Tomato	–	65.9	–	2.9
	100	160.9	95.0	2.6
Cabbage	–	4.2	–	2.5
	100	102.5	98.3	3.1
Garlic	–	ND	–	3.0
	100	103.7	103.7	2.8
Chicken liver	–	85.9	–	2.6
	100	180.1	94.2	3.1
Fish	–	74.2	–	2.6
	100	169.5	95.3	2.9

Table 7 . Results of HGAAS analysis of food samples spiked with known amounts of As(III). [a]Not determined.

Sample	Spiked (ng L^{-1})	Determined (ng L^{-1})	Recovery (%)	RSD (%)
Tap water	–	ND[a]	–	3.2
	50	47.9	95.8	3.3
	100	97.6	97.6	3.0
Well water	–	45.1	–	2.4
	50	93.7	97.2	2.7
	100	143.1	98.0	2.9
River water	–	ND		2.6
	50	48.1	96.2	2.8
	100	98.5	98.5	3.1
Waste water	–	125.6	–	3.0
	50	173.4	95.6	3.2
	100	222.5	96.9	3.4
Bottled water	–	ND	–	2.5
	50	51.2	102.4	2.7
	100	103.7	103.7	3.0

Table 8 . Results of HGAAS analysis of water samples spiked with known amounts of As(III). [a]not determined.

square interactions of variables, which are commonly ignored in univariate optimization. Our method possessed satisfactory sorbent capacity and lower RSD% in comparison with the most others methods. Other significant advantages of the proposed method were its low cost as well as rapid and simple separation.

Discussion

In summary, a new synthesized amphiphilic copolymer with pendant primary amine groups (PMaema) was prepared as solid-phase adsorbent. We used PMaema for the preconcentration of As(IIII) ions from the food samples and aqueous solution. Box–Behnken design was performed to optimize the experimental conditions. After microextraction, the amount of arsenic in the samples was measured through HGAAS technique. The adsorption of As(III) ions to the synthesized PMaema was also supported using computational chemistry studies. According to the solid phase adsorbent principle, the application of the amphiphilic copolymer during the

Sample	Microextraction procedure	Detection method	Linearity (ng L^{-1})	LOD (ng L^{-1})	RSD (%)	Sorbent capacity (mg g^{-1})	EF or PF	References
Food	CPE	HG-AFS	550–20,000	170	9.3		10.9	[2]
Rice	SPME	FI-HG AAS	1200–10,000	40	5.5	–	17	[50]
Water	SPME	GFAAS	1–20,000	87	4.5	15	13	[51]
Water	SPME	ICP-OES		150	4.3	55	–	[52]
Rice	CPE	ETAAS	50–10,000	10	2.5	–	73.8	[53]
Rice	MAS-LIS-DLLME	GFAAS	40–5000	5	3.7	–	10	[54]
Food and water	DES-VAME	HG AAS	15–150	7.5	2.7	–	85	[55]
Food and water	DES-UA-LPME	ETAAS	–	10	4.3	–	25	[38]
Food and water	SPME	HG-AAS	10–500	3.3	4.3	75.8	85/100	This study

Table 9. Comparison of the proposed method with other methods applied for preconcentration and determination of inorganic arsenic. *SPME* solid phase microextraction, *FI-HG AAS* Flow injection-hydride generation atomic absorption spectrometry, *GFAAS* graphite furnace atomic absorption spectrometry, *ICP-OES* inductively coupled plasma-optical emission spectrometry, *CPE* cloud point extraction, *ETAAS* Electrothermal atomic absorption spectrometry, *MAS-LIS-DLLME* fully-automated magnetic stirring-assisted lab-in-syringe dispersive liquid–liquid microextraction, *DES-VAME* deep eutectic solvent based vortex assisted microextraction, *DES-UA-LPME* deep eutectic solvent ultrasound-assisted liquid phase microextraction, *HG-AFS* hydride generation atomic fluorescence spectrometry.

Flame conditions	Arsenic	
Wavelength (nm)	197.2	
Lamp current (mA)	10	
Spectral bandwidth (nm)	0.2	
Temperature of quartz tube (°C)	900	
Air–acetylene flame (L min^{-1})	7.0	
Gas flow rates (L min^{-1})	1.5	
Hydride generation conditions	**Operating range**	**Optimized value**
1.0% (w/v) of $NaBH_4$ volume. mL	0.1–3	1.5
5.0 mol L^{-1} of HCl volume. mL	0.1–3	1.0
Argon flow rate. mL min^{-1}	50–200	120

Table 10. Optimal parameters of HG-AAS for the measurement of arsenic.

adsorption and desorption stages can obviously improve the recovery of As(III) ions. The optimized procedure was successfully applied to detect inorganic arsenic in the real samples, and displayed some advantages such as high sorbent capacity, cheapness, acceptable sensitivity, high precision, simplicity and environmental friendliness. Therefore, we consider that the optimized procedure is a competitive alternative for determining ultra-trace amounts of arsenic in real samples.

Materials and methods

Apparatus and software. The ultra-level of arsenic was determined by Hydride Generation Atomic Absorption Spectrometry (HG-AAS, Shimadzu AAS-6300 model, Kyoto, Japan). Measurement parameters of the HGAAS were operated lamp current at 10 mA, wavelength set at 197.2 nm, slit width set at 0.2 nm and air/acetylene flame at 4.66 L min^{-1}. The more detailed conditions were shown in Table 10. In the phase separation process, a centrifuge (320-Model Hettich Universal, Darmstadt, Germany) was applied. The vortex VG3 model (IKA GmbH, Germany) and microwave digestion (Milestone Ethos Easy Advanced, Italy) were utilized for desorption step and preparation of food samples, respectively. The pH of the working solutions was adjusted using a pH-meter (JP Selecta, Barcelona, Spain). Ultra-pure water with a resistivity of 18.2 MΩ was used in all experiments and was obtained from an Milli-Direct Q3 purification system (Millipore, Bedford, MA, USA). All optimization studies were conducted in triplicate and all results were averaged. Design-Expert trial version 12.0.1. (Stat-Ease Inc., Minneapolis) was used to generate the Box–Behnken design[39]. ^{1}H NMR spectrum of the copolymer (PMaema) was taken at 25 °C with an Agilent 600 MHz Nuclear Magnetic Resonance (NMR) (Agilent, Santa Clara, CA, USA) spectrometer equipped with a 3 mm broadband probe. FTIR spectrum of the

copolymer was recorded using Perkin-Elmer Spectrum 100 Fourier Transform Infrared (FTIR) spectroscopy (Perkin-Elmer Inc., Norwalk, CT, USA).

Reagents. Stock solution (1000 mg L^{-1}) of As(III) was prepared by dissolving the appropriate amount of Na_3AsO_3 (Sigma, St Louis, MO, USA). The calibration and working solutions were prepared by appropriate stepwise dilution of the stock solutions in 1.0% (w/v) of HCl solution. Ethanol, methanol, acetone, nitric acid, acetonitrile, hydrochloric acid, sulfuric acid, and tetrahydrofuran (THF) were purchased from Merck (Darmstadt, Germany). Methyl methacrylate (MMA), 2-aminoethyl methacrylate (aeMA) and 2,2′-azo bis isobutyronitrile (AIBN) used for synthesis of copolymers were purchased from Sigma-Aldrich (St. Louis, MO, USA). Acetate buffer solution (pH 4.3) was prepared with the appropriate mixture of sodium acetate and acetic acid in the water**.** To validate the data obtained from experimental measurements, two standard reference materials (SRMs) such as SRM 1573a (Tomato leaves) and SRM 1568a (Rice flour) were employed[3].

Sample collection. The applicability of the study was tested on food and water samples[3]. Food samples including rice, brown rice, carrot, pepper, flour, milk powder, tomato, cabbage, garlic, chicken liver and fish were collected randomly from local markets in Sivas, Turkey. Tap water was supplied from our laboratory. Bottled water was purchased from the market in Sivas, Turkey. Well water was collected from agricultural land in Sivas. The river water was collected from the surface of the Kızılırmak river passing through Sivas. The waste water was collected from the industrial area in Sivas.

Microwave digestion. The selected food samples and SRMs were prepared by closed-vessel microwave digestion[40]. At first, concentrated HNO_3 (6 mL) and concentrated H_2O_2 (2 mL) were added to 0.3 g of the samples in Teflon vessel and immediately placed in the microwave digestion system. The mixture solution was applied to a 2-step power (W) controlled program with a final step of 550 (W) (200 °C) for 10 min. After microwave digestion, the resulting solution were cooled and then transferred to polyethylene bottles. Finally, the obtained solution was completed to 100 mL with ultrapure water.

Synthesis of poly(methyl methacrylate-co-2-aminoethyl methacrylate copolymer (PMaema). A mixture of methyl methacrylate (MMA, 2.12 g), 2-aminoethyl methacrylate (aema, 4.03 g) and 2,2′-azo bis isobutyronitrile (AIBN, 0.016 g) was dissolved in 5 mL of DMF under argon[34]. The solution was kept at 80 °C for 60 min in an oil bath. Then, it was precipitated from distilled water (200 mL). Polymer recovered was washed with distilled water several times and dried under vacuum at 40 °C for 2 days. Yield was 4.06 g. PMMA homopolymer was synthesized using the same procedure with MMA monomer and AIBN only. Poly2aema homopolymer was synthesized using the same procedure with aema monomer and AIBN only.

Atomic model of PMaema. We considered molecule $C_{20}H_{36}N_2O_8$ as a model of PMaema polymer chain. The molecule includes four fragments; two of them are functionalized by NH_2 moieties[41]. Ends of the molecule are terminated by hydrogens to avoid dangling bonds. Optimized structure of the molecule was presented in Fig. 4. Note that the fragments with NH_2 moieties are almost parallel to each other, whereas two fragments without NH_2 form an obtuse angle.

Box–Behnken design. Experimental designs are widely used to reduce the number of optimization studies. Here, Box–Behnken design (BBD) based on response surface methodology (RSM) was continued with 30 combination runs of four experimental variables and 6 randomly distributed center points. The experimental variables included in the BBD were pH (A), PMaema amount (B), adsorption time (C) and ethanol volume (D), with each variable investigated at 3 levels comprising of low (− 1), mid. (0) and high (+ 1). The obtained model and results were given in Table 11. The mathematical relationship of the response (as absorbance) on the experimental variables can be approximated by the second order equation[42]:

$$y = b_0 + \sum_{i=1}^{k} b_i x_i + \sum_{i=1}^{k} b_{ii} x_1^2 + \sum_{1 \le i \le j}^{k} b_{ij}\, x_i\, x_j \quad (2)$$

where y was the absorbance; *Xi and Xj* were variables (i and j ranged from 1 to k); b_0 was constant term; b_i was linear coefficient, b_{ii} were interaction coefficient, and $_{bjj}$ was quadratic coefficient; k was number of independent variables (k = 4 in this study).

Details of density functional calculations. All calculations were performed with B3LYP exchange-corrected functional and 6–311 ++ G[2d,2p] electronic basic set[36]. We used the GPU-based TeraChem software[43]. Geometry optimizing was carried out with the efficient geomeTRIC energy minimizer[44]. To take into account non-covalent interactions, the dispersion corrections D3 proposed by Grimme[45] were included. Solvent effects were introduced in the frame of the COSMO solvent model[46] implemented in TeraChem. The dielectric constant of the solvent (acidic ethanol) was chosen to be equal to 25.3. Chemical reactivity descriptors such as chemical potential (μ), electronegativity (χ), hardness (η) and softness (σ) were calculated using ground state ionization energy (I) and electron affinity (A). The relations between total electronic energy (E), number of electrons (N), ionization energy and electron affinity and quantum descriptors mentioned above were given via the following equations;

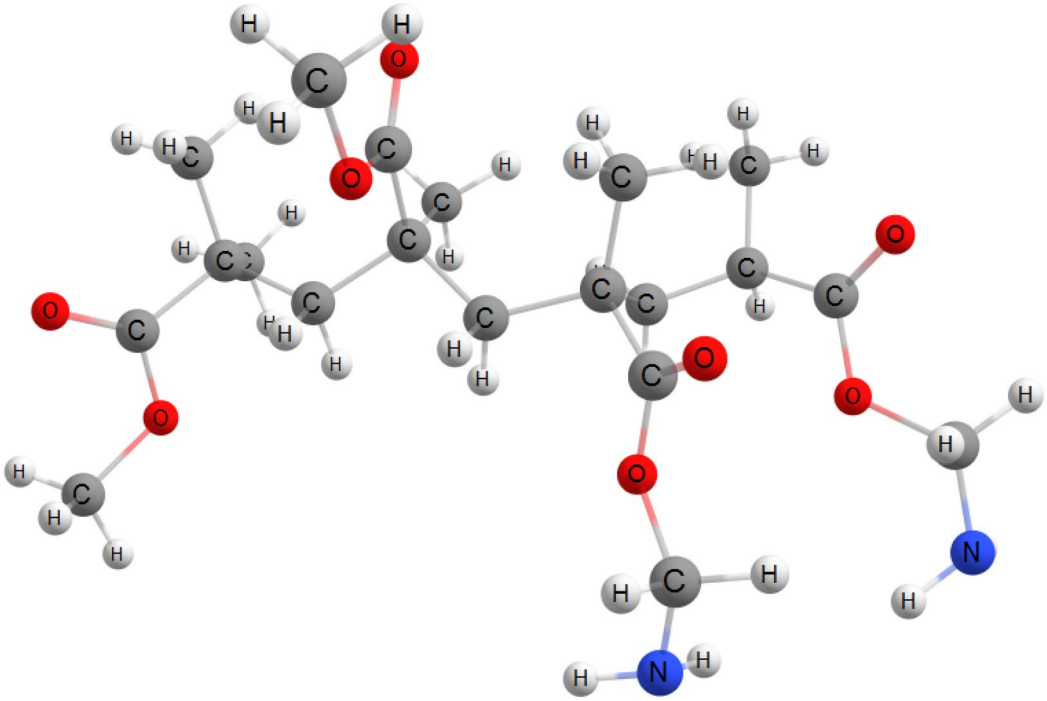

Figure 4. Optimized geometry of the $C_{20}H_{36}N_2O_8$ molecule used as a model of PMmae polymer chain.

$$\mu = -\chi = \left[\frac{\partial E}{\partial N}\right]_{v(r)} = -\left(\frac{I+A}{2}\right) \tag{3}$$

$$\eta = \left[\frac{\partial^2 E}{\partial N^2}\right]_{v(r)} = \frac{I-A}{2} \tag{4}$$

$$\sigma = 1/\eta \tag{5}$$

The I and A values can be evaluated from frontier orbitals energies in accordance with the Koopmans theorem. Parr et al.[47] proposed the electrophilicity index ω based on electronegativity and absolute hardness values of chemical species. Chattaraj defined the nucleophilicity index ε. These indexes were calculated as

$$\omega = \chi^2/2\eta \tag{6}$$

$$\varepsilon = 1/\omega \tag{7}$$

In recent years, Gazquez et al.[48] introduced electrodonating power (ω^-) and electroaccepting powers (ω^+). These parameters predict electron donating and electron accepting capabilities of molecule, respectively. They were calculated from I and A with the following equations:

$$\omega^+ = (I+3A)^2/(16(I-A)) \tag{8}$$

$$\omega^- = (3I+A)^2/(16(I-A)) \tag{9}$$

Optimized solid phase microextraction. The experimental steps of the optimized SPME method were carried out as follows. Initially, 110 mg of the PMaema was exactly weighed, and added to 30 mL of sample solution containing 40 ng L^{-1} of As(III) into a 50 mL-centrifuge tube. Then, acetate buffer solution was added to the solution to obtain pH of 4.3. The resulting mixture was kept on an orbital shaker for 22 min to accelerate the mass transfer of the As(III) from the sample solution to the solid adsorbent. The extracted As(III) on the PMaema was separated from the sample solution by centrifugation (4000 rpm, 5 min), and subsequently aqueous phase was emptied by Pasteur pipette. Next, in order to elute the adsorbed As(III) on the PMaema, 1.5 mL of ethanol (as an eluent solvent) was added to the remaining solid phase. Finally, the amount of arsenic in eluted solution was determined by HG-AAS[49]. The sample blanks were prepared in the same manner. All experiments were repeated three times.

Factors		Symbol	Levels of factors		
			Low	Middle	High
pH		A	2.5	5.25	8
PMaema amount (mg)		B	5	77.5	150
Adsorption time (min)		C	0	15	30
Ethanol volume (mL)		D	0.2	1.1	2
Run	***A***	***B***	***C***	***D***	**Recovery (%)**
1	5.25	150	0	1.1	52.6
2	8	77.5	30	1.1	64.4
3	5.25	77.5	30	0.2	47.1
4	5.25	150	15	2	71.5
5	8	77.5	15	2	55.9
6	5.25	77.5	15	1.1	90.8
7	5.25	77.5	30	2	82.6
8	8	77.5	0	1.1	38.1
9	2.5	5	15	1.1	52.3
10	5.25	77.5	15	1.1	92.1
11	8	5	15	1.1	49.3
12	5.25	150	30	1.1	91.5
13	2.5	150	15	1.1	74.4
14	5.25	5	15	2	62.2
15	2.5	77.5	30	1.1	71.1
16	2.5	77.5	15	2	74.6
17	5.25	77.5	15	1.1	89.4
18	5.25	77.5	0	2	56.8
19	8	150	15	1.1	58.6
20	5.25	5	30	1.1	53.4
21	2.5	77.5	0	1.1	50.4
22	5.25	77.5	15	1.1	91.4
23	5.25	77.5	0	0.2	41.1
24	2.5	77.5	15	0.2	39.8
25	5.25	77.5	15	1.1	84.4
26	8	77.5	15	0.2	45.9
27	5.25	150	15	0.2	60.4
28	5.25	5	15	0.2	36.7
29	5.25	77.5	15	1.1	92.6
30	5.25	5	0	1.1	52.8

Table 11. Factors their symbols levels design matrix and results in the BBD to evaluate the microextraction method.

Received: 1 November 2020; Accepted: 8 February 2021
Published online: 09 March 2021

References

1. Munonde, T. S., Maxakato, N. W. & Nomngongo, P. N. Preparation of magnetic Fe_3O_4 nanocomposites modified with MnO_2, Al_2O_3, Au and their application for preconcentration of arsenic in river water samples. *J. Environ. Chem. Eng.* **6**, 1673–1681 (2018).
2. Castor, J. M. R. *et al.* An evaluation of the bioaccessibility of arsenic in corn and rice samples based on cloud point extraction and hydride generation coupled to atomic fluorescence spectrometry. *Food Chem.* **204**, 475–482 (2016).
3. Gurkan, R., Kır, U. & Altunay, N. Development of a simple, sensitive and inexpensive ion-pairing cloud point extraction approach for the determination of trace inorganic arsenic species in spring water, beverage and rice samples by UV–Vis spectrophotometry. *Food Chem.* **180**, 32–41 (2015).
4. Oksüz, N., Saçmacı, S., Saçmacı, M. & Ulgen, A. A new fluorescence reagent: Synthesis, characterization and application for speciation of arsenic (III)/(VI) species in tea samples. *Food Chem.* **270**, 579–584 (2019).
5. Erdogan, H., Yalçınkaya, O. & Turker, A. R. Determination of inorganic arsenic species by hydride generation atomic absorption spectrometry in water samples after preconcentration/separation on nano ZrO_2/B_2O_3 by solid phase extraction. *Desalination* **280**, 391–396 (2011).
6. Lynch, H. N., Greenberg, G. I., Pollock, M. C. & Lewis, A. S. A comprehensive evaluation of inorganic arsenic in food and considerations for dietary intake analyses. *Sci. Total Environ.* **496**, 299–313 (2014).
7. Zou, H. *et al.* Occurrence, toxicity, and speciation analysis of arsenic in edible mushrooms. *Food Chem.* **281**, 269–284 (2019).
8. Bralatei, E., Lacan, S., Krupp, E. M. & Feldmann, J. Detection of inorganic arsenic in rice using a field test kit: A screening method. *Anal. Chem.* **87**(22), 11271–11276 (2015).

9. WHO Guidelines for Drinking Water Quality. *Volume 1, Recommendation* (World Health Organization, 2008).
10. TFC. *Setting Maximum Levels for Certain Contaminants in Foodstuffs*. Turkish Food Codex 2002/63 (2002).
11. Lee, H. G., Kwon, J. Y. & Chung, D. S. Sensitive arsenic speciation by capillary electrophoresis using UV absorbance detection with on-line sample preconcentration techniques. *Talanta* **181**, 366–372 (2018).
12. Chen, S., Li, J., Lu, D. & Zhang, Y. Dual extraction based on solid phase extraction and solidified floating organic drop microextraction for speciation of arsenic and its distribution in tea leaves and tea infusion by electrothermal vaporization ICP-MS. *Food Chem.* **211**, 741–747 (2016).
13. Shirani, M., Habibollahi, S. & Akbari, A. Centrifuge-less deep eutectic solvent based magnetic nanofluid-linked airagitated liquid–liquid microextraction coupled with electrothermal atomic absorption spectrometry for simultaneous determination of cadmium, lead, copper, and arsenic in food samples and non-alcoholic beverages. *Food Chem.* **281**, 304–311 (2019).
14. Shirani, M., Semnani, A., Habibollahi, S. & Haddadi, H. Ultrasound-assisted, ionic liquid-linked, dual-magnetic multiwall carbon nanotube microextraction combined with electrothermal atomic absorption spectrometry for simultaneous determination of cadmium and arsenic in food samples. *J. Anal. At. Spectrom.* **30**, 1057–1063 (2015).
15. Vicente-Martinez, Y., Caravaca, M. & Soto-Meca, A. Non-chromatographic speciation of arsenic by successive dispersive liquid liquid microextraction and in situ formation of an ionic liquid in water samples. *Microchem. J.* **157**, 105102 (2020).
16. Vera, R. *et al.* Automatic determination of arsenate in drinking water by flow analysis with dual membrane-based separation. *Food Chem.* **283**, 232–238 (2019).
17. Najafi, A. & Hashemi, M. Vortex-assisted supramolecular solvent microextraction based on solidification of floating drop for preconcentration and speciation of inorganic arsenic species in water samples by molybdenum blue method. *Microchem. J.* **150**, 104102 (2019).
18. Dos Santos, Q. O., Silva Junior, M. M., Lemos, V. A., Ferreira, S. L. C. & de Andrade, J. B. An online preconcentration system for speciation analysis of arsenic in seawater by hydride generation flame atomic absorption spectrometry. *Microchem. J.* **143**, 175–180 (2018).
19. Jalilian, R., Shahmari, M., Taheri, A. & Gholami, K. Ultrasonic-assisted micro solid phase extraction of arsenic on a new ionim-printed polymer synthesized from chitosan-stabilized pickering emulsion in water, rice and vegetable samples. *Ultrason. Sonochem.* **61**, 104802 (2020).
20. Majumder, S., Margui, E., Roman-Ross, G., Chatterjee, D. & Hidalgo, M. Hollow fiber liquid phase microextraction combined with total reflection X-ray fluorescence spectrometry for the determination of trace level inorganic arsenic species in waters. *Talanta* **217**, 121005 (2020).
21. Fiorentini, E. F., Canizo, B. V. & Wuilloud, R. G. Determination of As in honey samples by magnetic ionic liquid-based dispersive liquid-liquid microextraction and electrothermal atomic absorption spectrometry. *Talanta* **198**, 146–153 (2019).
22. Yilmaz, E. Use of hydrolytic enzymes as green and effective extraction agents for ultrasound assisted-enzyme based hydrolytic water phase microextraction of arsenic in food samples. *Talanta* **189**, 302–307 (2018).
23. Zhao, L. *et al.* Preparation of thiol- and amine-bifunctionalized hybrid monolithic column *via* "one-pot" and applications in speciation of inorganic arsenic. *Talanta* **192**, 339–346 (2019).
24. Omidi, F., Behbahani, M., Khadem, M., Golbabaei, F. & Shahtaheri, S. J. Application of a new sample preparation method based on surfactant-assisted dispersive micro solid phase extraction coupled with ultrasonic power for easy and fast simultaneous pre-concentration of toluene and xylene biomarkers from human urine samples. *J. Iran. Chem. Soc.* **16**(6), 1131–1138 (2019).
25. Behbahani, M., Bagheri, S., Omidi, F. & Amini, M. M. An amino-functionalized mesoporous silica (KIT-6) as a sorbent for dispersive and ultrasonication-assisted micro solid phase extraction of hippuric acid and methylhippuric acid, two biomarkers for toluene and xylene exposure. *Microchim. Acta* **185**(11), 505 (2018).
26. Omidi, F., Dehghani, F. & Shahtaheri, S. J. N-doped mesoporous carbon as a new sorbent for ultrasonic-assisted dispersive micro-solid-phase extraction of 1-naphthol and 2-naphthol, the biomarkers of exposure to naphthalene, from urine samples. *J. Chromatogr. B* **1160**, 122353 (2020).
27. Behbahani, M., Zarezade, V., Veisi, A., Omidi, F. & Bagheri, S. Modification of magnetized MCM-41 by pyridine groups for ultrasonic-assisted dispersive micro-solid-phase extraction of nickel ions. *Int. J. Environ. Sci. Technol.* **16**(10), 6431–6440 (2019).
28. Ali, J., Tuzen, M., Kazi, T. G. & Hazer, B. Inorganic arsenic speciation in water samples by miniaturized solid phase microextraction using a new polystyrene polydimethyl siloxane polymer in micropipette tip of syringe system. *Talanta* **161**, 450–458 (2016).
29. Yildiz, U., Hazer, B. & Tauer, K. Tailoring polymer architectures with macromonomer azoinitiators. *Polym. Chem.* **3**(5), 1107–1118 (2012).
30. Balcı, M. *et al.* Synthesis and characterization of novel comb-type amphiphilic graft copolymers containing polypropylene and polyethylene glycol. *Polym. Bull.* **64**(7), 691–705 (2010).
31. Ji, W., Panus, D., Palumbo, R. N., Tang, R. & Wang, C. Poly(2-aminoethyl methacrylate) with well-defined chain length for DNA vaccine delivery to dendritic cells. *Biomacromol* **12**, 4373–4385 (2011).
32. He, L., Read, E. S., Armes, S. P. & Adams, D. J. Direct synthesis of controlled-structure primary amine-based methacrylic polymers by living radical polymerization. *Macromolecules* **40**(13), 4429–4438 (2007).
33. Mendonça, P. V. *et al.* Straightforward ARGET ATRP for the synthesis of primary amine polymethacrylate with improved chain-end functionality under mild reaction conditions. *Macromolecules* **47**, 4615–4621 (2014).
34. Hazer, B. Macrointermediates for block and graft copolymers. In *Handbook of Engineering Polymeric Materials* (ed. Cheremisinoff, N. P.) 725–734 (Marcel Dekker, 1997).
35. Ghadban, A., Reynaud, E., Rinaudo, M. & Albertin, L. RAFT copolymerization of alginate-derived macromonomers–synthesis of a well-defined poly (HEMAm)-graft-(1 → 4)-α-l-guluronan copolymer capable of ionotropic gelation. *Polym. Chem.* **4**(17), 4578–4583 (2013).
36. Pearson, R. G. Hard and soft acids and bases. *J. Am. Chem. Soc.* **85**(22), 3533–3539 (1963).
37. Islam, N. & Kaya, S. (eds) *Conceptual Density Functional Theory and Its Application in the Chemical Domain* (CRC Press, 2018).
38. Zounr, R. A., Tuzen, M. & Khuhawar, M. Y. Ultrasound assisted deep eutectic solvent based on dispersive liquid liquid microextraction of arsenic speciation in water and environmental samples by electrothermal atomic absorption spectrometry. *J. Mol. Liq.* **242**, 441–446 (2017).
39. Altunay, N. *et al.* Spectrophotometric determination of aflatoxin B1 in food sample: Chemometric optimization and theoretical supports for reaction mechanisms and binding regions. *J. Food Compos. Anal.* **94**, 103646 (2020).
40. Zhang, N. *et al.* Simultaneous determination of arsenic, cadmium and lead in plant foods by ICP-MS combined with automated focused infrared ashing and cold trap. *Food Chem.* **264**, 462–470 (2018).
41. Lee, C., Yang, W. & Parr, R. G. Development of the Colle-Salvetti correlation-energy formula into a functional of the electron density. *Phys. Rev. B* **37**(2), 785 (1988).
42. Sy Mohamad, S. F., Mohd Said, F., Abdul Munaim, M. S., Mohamad, S. & Azizi Wan Sulaiman, W. M. Application of experimental designs and response surface methods in screening and optimization of reverse micellar extraction. *Crit. Rev. Biotechnol.* **40**(3), 341–356 (2020).
43. Titov, A. V., Ufimtsev, I. S., Luehr, N. & Martinez, T. J. Generating efficient quantum chemistry codes for novel architectures. *J. Chem. Theory Comput.* **9**(1), 213–221 (2013).
44. Wang, L. P. & Song, C. Geometry optimization made simple with translation and rotation coordinates. *J. Chem. Phys.* **144**(21), 214108 (2016).

45. Grimme, S., Antony, J., Ehrlich, S. & Krieg, H. A consistent and accurate ab initio parametrization of density functional dispersion correction (DFT-D) for the 94 elements H-Pu. *J. Chem. Phys.* **132**(15), 154104 (2010).
46. Liu, F., Luehr, N., Kulik, H. J. & Martínez, T. J. Quantum chemistry for solvated molecules on graphical processing units using polarizable continuum models. *J. Chem. Theory Comput.* **11**(7), 3131–3144 (2015).
47. Parr, R. G., Szentpaly, L. V. & Liu, S. Electrophilicity index. *J. Am. Chem. Soc.* **121**(9), 1922–1924 (1999).
48. Morell, C., Gázquez, J. L., Vela, A., Guégan, F. & Chermette, H. Revisiting electroaccepting and electrodonating powers: Proposals for local electrophilicity and local nucleophilicity descriptors. *Phys. Chem. Chem. Phys.* **16**(48), 26832–26842 (2014).
49. Schlotthauer, J. *et al.* Determination of inorganic arsenic in Argentinean rice by selective HGAAS: Analytical performance for paddy, brown and polished rice. *J. Food Compos. Anal.* **1**, 103506 (2020).
50. dos Santos Costa, B. E. & Coelho, N. M. M. Selective determination of As (III) and total inorganic arsenic in rice sample using in-situ μ-sorbent formation solid phase extraction and FI-HG AAS. *J. Food Compos. Anal.* **95**, 103686 (2020).
51. Wang, Q., Yu, Z., Lan, J., Liu, A. & Tian, Y. Bifunctional magnesium oxide crystal successively as adsorbent and matrix modifier for preconcentration and determination of arsenic by graphite furnace atomic absorption spectrometry. *Microchem. J.* **133**, 412–416 (2017).
52. Dados, A., Kartsiouli, E., Chatzimitakos, T., Papastephanou, C. & Stalikas, C. D. In situ trapping of As, Sb and Se hydrides on nanometer-sized ceria-coated iron oxide–silica and slurry suspension introduction to ICP-OES. *Talanta* **130**, 142–147 (2014).
53. dos Santos Costa, B. E., Coelho, N. M. M. & Coelho, L. M. Determination of arsenic species in rice samples using CPE and ETAAS. *Food Chem.* **178**, 89–95 (2015).
54. Wang, X. *et al.* Fully-automated magnetic stirring-assisted lab-in-syringe dispersive liquid–liquid microextraction for the determination of arsenic species in rice samples. *RSC Adv.* **8**(30), 16858–16865 (2018).
55. Altunay, N., Elik, A. & Gürkan, R. Innovative and practical deep eutectic solvent based vortex assisted microextraction procedure for separation and preconcentration of low levels of arsenic and antimony from sample matrix prior to analysis by hydride generation-atomic absorption spectrometry. *Food Chem.* **293**, 378–386 (2019).

Acknowledgements

Dr. Mustafa Tuzen thanks to Turkish Academy of Sciences for financial support. This work was partly supported by the Kapadokya University Research Funds (#KÜN.2020BAGP-001).

Author contributions

A.E.: Supervision, Software. M.T.: Investigation, Validation. B.H.: Supervision, Software. S.K.: Conceptualization, Writing- Reviewing. K.P.K.: Supervision, Software, Investigation. N.A.: Original draft preparation, Writing-Reviewing, Software, Experiments.

Competing interests

The authors declare no competing interests.

Additional information

Correspondence and requests for materials should be addressed to M.T. or N.A.

Reprints and permissions information is available at www.nature.com/reprints.

Publisher's note Springer Nature remains neutral with regard to jurisdictional claims in published maps and institutional affiliations.